Cytomegalovirus-encoded immediate early 1 protein perturbs neural progenitor proliferation *via* interfering with host PML–DISC1 interaction

Received for publication, September 1, 2025, and in revised form, January 9, 2026 Published, Papers in Press, February 6, 2026
https://doi.org/10.1016/j.jbc.2026.111269

Atsushi Saito[1,2,‡], Stephanie Tankou[2,‡], Kazuhiro Ishii[2,‡], Makiko Sakao-Suzuki[3,4,‡], Edwin C. Oh[5,‡], Hannah Murdoch[6], Ho Namkung[2], Sunday Adelakun[2], Keiko Furukori[2], Masahiro Fujimuro[7], Paolo Salomoni[8], Gerd G. Maul[9], Gary S. Hayward[10], Qiyi Tang[11], Robert H. Yolken[12], Miles D. Houslay[13], Nicholas Katsanis[14], Isao Kosugi[3], Kun Yang[2], Atsushi Kamiya[2], Koko Ishizuka[2], and Akira Sawa[1,2,15,16,17,*]

From the [1]Department of Neuroscience, and [2]Department of Psychiatry, Johns Hopkins University School of Medicine and Bloomberg School of Public Health, Baltimore, USA; [3]Department of Regenerative & Infectious Pathology, and [4]Department of Neurology, Hamamatsu University School of Medicine, Hamamatsu, Japan; [5]Nevada Institute of Personalized Medicine, University of Nevada, Las Vegas, Nevada, USA; [6]Molecular Pharmacology Group, Institute of Neuroscience and Psychology, University of Glasgow, Glasgow, UK; [7]Department of Cell Biology, Kyoto Pharmaceutical University, Kyoto, Japan; [8]Nuclear Function in CNS Pathophysiology, German Center for Neurodegenerative Diseases, Bonn, Germany; [9]The Wistar Institute, Philadelphia, Pennsylvania, USA; [10]Department of Oncology, Johns Hopkins University School of Medicine and Bloomberg School of Public Health, Baltimore, USA; [11]Department of Microbiology, Howard University College of Medicine, Washington, District of Columbia, USA; [12]Department of Pediatrics, Johns Hopkins University School of Medicine and Bloomberg School of Public Health, Baltimore, USA; [13]Institute of Pharmaceutical Science, King's College London, London, UK; [14]Rescindo Therapeutics Inc, Cary, North Carolina, USA; [15]Department of Biomedical Engineering, [16]Department of Genetic Medicine, and [17]Department of Mental Health, Johns Hopkins University School of Medicine and Bloomberg School of Public Health, Baltimore, USA

Reviewed by members of the JBC Editorial Board. Edited by Craig Cameron

Congenital cytomegalovirus (CMV) infection is the most common perinatal infection, affecting up to 0.5% of infants. This elicits long-term disabilities that include neuropsychiatric manifestations, such as intellectual disability, microcephaly. Despite its high prevalence, the underlying mechanism of how congenitally acquired CMV infection causes brain pathology remain unknown. Here, we discovered the molecular interplay of key host (DISC1 and promyelocytic leukemia [PML]) and viral (immediate early 1 [IE1]) proteins within the neural progenitor cells, which underlay an attenuated neural progenitor proliferation in congenital CMV infection. Abolishing the viral IE1 protein by delivering IE1-targeting CRISPR/Cas9 to fetal brain rescued this progenitor cell deficit, a key pathology in congenital CMV infection. A selective targeting to a viral-specific protein by the CRISPR/Cas9 system is minimal in off-target effects. We further observed that CMV-encoded IE1 protein interferes with host PML–DISC1 interaction, resulting in disturbance of the Notch pathway *in vitro* and in embryonic brains. Therefore, we believe that a pivotal role of IE1 in an attenuated neural progenitor proliferation in the developing cortex through its interfering with interaction between host DISC1 and PML proteins.

Congenital cytomegalovirus (CMV) infection is the most common perinatal infection, affecting up to 0.5% of infants (https://www.cdc.gov/cytomegalovirus/about/). About 10% of infected babies are symptomatic at birth, and many will suffer from permanent sequelae, including: intellectual disability, microcephaly, neuromotor deficits, and hearing loss, which remains a major medical and public health issue (1–6). The epidemiological patterns of congenital CMV infection differ according to socioeconomic status (7), and CMV infection indeed exerts a pronounced burden in developing countries. For example, pregnant females suffering from infectious diseases, such as HIV, are at high risk (8–12). In the United States, the incidence of long-term sequelae from congenital CMV infection is greater than those from other perinatal complications, such as fetal alcohol syndrome and neural tube defects (13). Despite its high prevalence, the underlying mechanisms of how congenitally acquired CMV infection causes brain pathology remain unknown, resulting in limited means for prevention and treatments (1).

There have been major efforts to develop a vaccine to prevent the transmission of CMV from pregnant mothers to their offspring. Immunoglobulin therapy can decrease the severity of disabilities caused by fetal CMV infection after a primary maternal infection during pregnancy (14). However, congenital CMV infection following nonprimary maternal infection accounts for a majority of congenital CMV infections (15, 16). For babies with signs of congenital CMV infection at birth, antiviral medications (*e.g.*, ganciclovir and valganciclovir) may improve hearing and developmental outcomes. Nevertheless, a major remaining question is whether this postnatal treatment

‡ These authors contributed equally to this work.
* For correspondence: Akira Sawa, asawa1@jhmi.edu.

may correct the brain anomalies that happen before birth, which result in intellectual disability and long-term neuropsychiatric problems. Potential side effects of these therapies also limit their widespread application. To overcome these dilemmas, an establishment of a vaccine against CMV is awaited: a current field consensus is that a safe and effective human CMV (HCMV) vaccine is within reach and that even a partially effective vaccine would have a major effect on the global health consequences of HCMV infection (17).

In many diseases, building animal models is an essential process to understand their pathological mechanisms, in particular when we wish to establish causality (18). Because of the abundance of experimental tools, mouse models are widely used (19). Indeed, to study congenital CMV infection, there are multiple mouse models (20–27). To overcome the placental barrier is refractory to CMV transmission in mice, severe combined immunodeficient mice have been used (20). There have been multiple reports that use newborn mice and built a perinatal CMV infection model (21–23). More recently, pioneering effort of delivering murine CMV (MCMV) *in utero* has also been published, in which direct injection of MCMV into the placenta or even more directly into the fetal brains (ventricles) was made (24, 25, 27). An alternate strategy is to use guinea pig for building the model because guinea pig CMV can cross the placenta and cause infection *in utero* (28). Through these efforts, the link between CMV infection and histoanatomical/behavioral changes has been productively addressed. Nevertheless, the intracellular signaling mechanisms affected by viral infection are understudied.

In the present study, we studied an alteration in molecular signaling in neural progenitor cells (NPCs) in congenital MCMV infection. Although the prenatal influence of CMV on NPCs and its impact on a long-term disability with intellectual disability has been suggested (29–32), the molecular mechanism of the host–viral interaction remains unknown. In our present efforts, we pinned down that viral-encoded immediate early 1 (IE1) interferes with host protein signaling essential for proper maintenance of NPCs in the prenatal brain through the application of the CRISPR/Cas9 system against the CMV-encoded IE1.

Results

Mouse models for congenital CMV infection

C57BL/6 mice are well characterized in many behavioral studies (33), whereas this strain is known to have CMV-resistant haplotypes associated with the natural killer cell activation in the uterus (34–36). The pioneering studies that used mouse CMV for the injection to the placenta or the fetal brains were conducted with an outbred strain Institute of Cancer Research (25). Nevertheless, given the high utility of C57BL/6 mice because of the access to many genetically engineered lines and the abundance of referential behavioral/neurobiological data and protocols, the use of C57BL/6 mice may be scientifically meaningful (27). Accordingly, by optimizing the timing of viral injection to minimize the resistance, we injected CMV in C57BL/6 mice at embryonic day 14.5 (E14.5), with safe delivery of pups after the survival surgery.

We first used an intraplacental injection model (P-inj model) in which MCMV was intraplacentally injected at E14.5. Viral-encoded IE1 protein has pivotal roles in acute CMV infection by initiation of the viral replication (37, 38), and IE1 immunostaining is widely used for the evidence of CMV infection in humans and animal models (39). IE1 immuno-positive cells were observed throughout the fetal brain, when we segmented the brain in several gross regions (Fig. 1*A*). In the developing cerebral cortex, most of the MCMV-infected cells were in the ventricular zone/subventricular zone (VZ/SVZ), a proliferative compartment in the developing brain (Fig. 1*B*), as is evident in the human pathology (29). About 90% of IE1-positive cells inside the MCMV-infected foci in the VZ/SVZ were costained with Sox2, a representative marker for NPCs (Fig. S1). Together, by adjusting the injection date to E14.5, P-inj model seems to satisfy construct and face validity at the reasonable level, without affecting stable production and survival rates.

P-inj model includes some potential limitation: the infected cells in the brain were relatively sparse, which may not be optimal when intensive characterization and intervention are performed at the cellular levels. Thus, we introduced a complementary model, in which MCMV was directly injected into the lateral ventricle of embryos at E14.5 (Fig. 1*C*). Many groups including ours have utilized *in utero* gene transfer to provide plasmids to modulate gene expression in the developing cortex (40), and we applied this methodology for viral transfer. In the ventricular injection model (V-inj model), infected IE1-positive cells were observed throughout the fetal brain, including the cerebral cortex, which is much denser than those in P-inj model (Fig. 1*C*). Nevertheless, these two different models (P-inj and V-inj models) showed a similar infection pattern in which most of the MCMV-infected cells were in the VZ/SVZ, a proliferative compartment in the developing brain (Fig. 1*D*). Taken together, we conclude that V-inj model may be a useful alternate model to P-inj model, in particular when higher density of MCMV-infected cells is more advantageous for assays.

NPC proliferation deficits in the developing cortex and behavioral changes in congenital CMV mouse models

The distribution of CMV in the VZ/SVZ prompted us to ask whether the viral infection might elicit defects in NPC proliferation (41), which can underlie brain anomalies and intellectual disability (42). To evaluate this possibility, by using both models, we pulse-labeled pregnant dams with bromodeoxyuridine/5-bromo-2′-deoxyuridine (BrdU) 2 h before euthanizing the animals on E16.5. Analysis of cortical sections revealed that BrdU signal intensity, a marker for proliferating cells, in IE1-positive cells were significantly lower than that in IE1-negative cells inside the cerebral MCMV-infected foci in both models (Fig. 2*A* and S2*A*). These results indicate that cellular proliferation is suppressed in IE1-positive (MCMV-infected) NPCs.

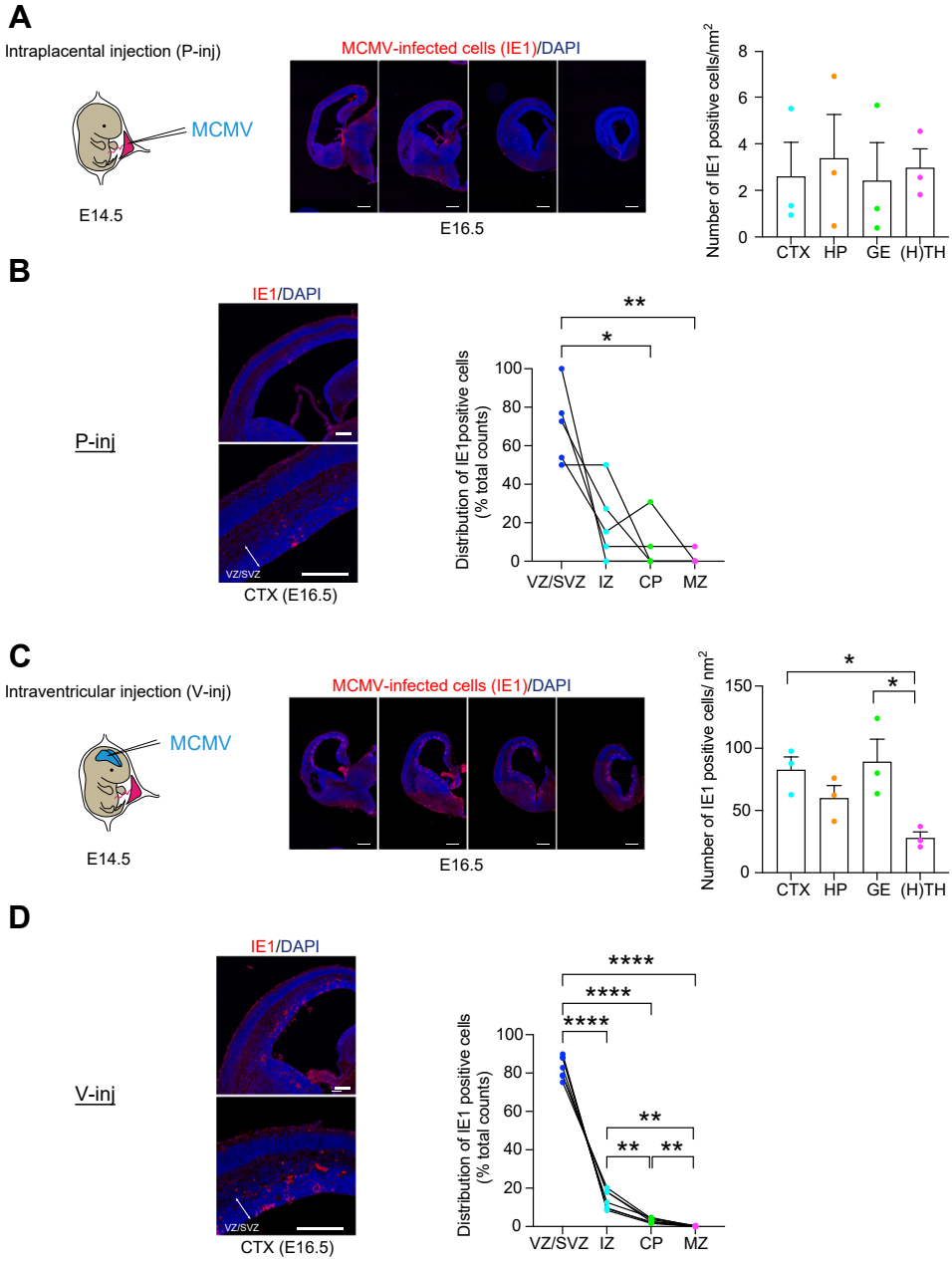

Figure 1. Histological validation of intraplacental (P-inj) and intraventricular (V-inj) injection models. *A,* E14.5 embryos were intraplacentally (P-inj) injected with MCMV. Immunostaining for IE1 (*red*), 2 days after injection (E16.5), shows a focus of MCMV-infected cells throughout the developing brains. Sequential infected-brain images show distribution of IE1-positive cells (*red*) in the intraplacental (P-inj) injection models. Graphs show density of IE1-positive cells in four brain regions: cortex (CTX), hippocampus (HP), ganglionic eminence (GE), as well as thalamus and hypothalamus [H(TH)]. Scale bars represent 500 μm. Graphs show mean +/− SEM (n = 3 mice, 12–15 slices per mouse; one-way ANOVA: F(3,8) = 0.080, $p = 0.969$). *B,* cortical distribution of IE1 cells in P-inj model. Immunostaining for IE1 (*red*), 2 days after injection (E16.5), shows a focus of MCMV-infected cells in the cortex. Graphs show the pattern of distribution (ratio) in the cortex: ventricular zone/subventricular zone (VZ/SVZ), intermediate zone (IZ), cortical plate (CP), and marginal zone (MZ). In the developing cerebral cortex, most of the MCMV-infected cells were in the VZ/SVZ. The *dots* connected with a line indicate the data from the identical brain. Scale bars represent 200 μm. [n = 5 mice, Tukey's multiple comparison test *$p < 0.05$, **$p < 0.01$; repeated measures one-way ANOVA: layer (between columns) F(1.715,6.859) = 15.21, $p = 0.004$; individual (between columns) F(4,12) = 2.463e-21, $p > 0.999$]. *C,* E14.5 embryos were intracranially (V-inj) injected with MCMV. Immunostaining for IE1 (*red*), 2 days after injection (E16.5), shows a focus of MCMV-infected cells throughout the developing brains. Sequential infected-brain images show distribution of IE1-positive cells (*red*) in the intracranially (V-inj) injection models. Graphs show density of IE1-positive cells in four brain regions, indicating that IE1-positive cells appear much more densely in V-inj model compared with those in P-inj model. Furthermore, they appear more densely in CTX and GE, compared with H(TH). Scale bars represent 500 μm. Graphs show mean +/− SEM (n = 3 mice, 12–15 slices per mouse, Tukey's multiple comparison test *$p < 0.05$; one-way ANOVA: F(3,8) = 5.468, $p = 0.024$). *D,* cortical distribution of IE1 cells in V-inj model. Immunostaining for IE1 (*red*), 2 days after injection (E16.5), shows a focus of MCMV-infected cells in the cortex. Graphs show the pattern of distribution (ratio) in the cortex: VZ/SVZ, IZ, CP, and MZ. In the developing cerebral cortex, most of the MCMV-infected cells were in the VZ/SVZ. The *dots* connected with a line indicate the data from the identical brain. Scale bars represent 200 μm. [n = 7 mice, Tukey's multiple comparison test **$p < 0.01$, ****$p < 0.0001$; Repeated measures one-way ANOVA: layer (between columns) F(1.039,6.236) = 551.8, $p < 0.0001$; individual (between rows) F(6,18) = 7.471e-20, $p > 0.999$]. E16.5, embryonic day 16.5; E15.5, embryonic day 15.5; IE1, immediate early 1.

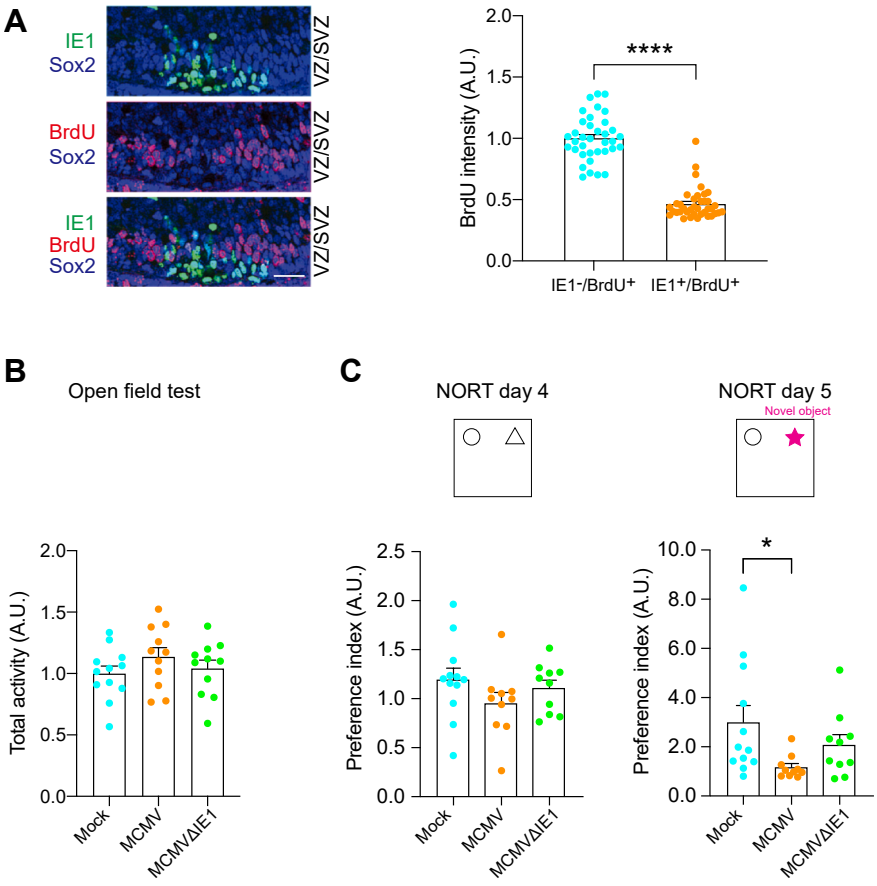

Figure 2. Intraplacental injection (P-inj) model shows impairment of neuronal development and a cognitive deficit. *A,* immunostaining for IE1 (*green*) and BrdU (*red*) shows a decrease in BrdU-labeled cells in MCMV-infected areas. IE1-positive nuclei rarely merged with BrdU-positive nuclei in P-inj model. The scale bar represents 50 μm. Graph shows BrdU incorporation in uninfected NPC (Sox2-positive but IE1-negative) and infected NPC (Sox2- and IE1-double positive). The ratio of BrdU- and Sox2-double positive nuclei to total Sox2-positive nuclei was significantly decreased in the infected area compared to the uninfected area. *Blue*, Sox2; *green*, IE1; *red*, BrdU. Graph shows mean +/− SEM (n = 36–55 cells per group, $^{****}p < 0.0001$; Mann–Whitney test). *B,* the total activity of mice intraplacentally infected with mock, MCMV, and MCMV IE1-deletion mutant (MCMV-ΔIE1) (P-inj) in the open field test. Total activity was not significantly different between groups. (Mock: n = 12 MCMV: n = 11, MCMVΔIE1: n = 11; one-way ANOVA: $F(2,31) = 1.036$, $p = 0.367$). *C,* the results of the novel object recognition test (NORT) in three groups (mock, MCMV, and MCMVΔIE1). Preference index (novel object exploration time/exploration time of both objects) was significantly decreased (impairment of object recognition memory) in MCMV-infected mice compared to control mice (mock) (day5). When mice were infected with MCMVΔIE1, such impairment of object recognition memory was not observed (day 5). Graphs show mean +/− SEM (mock: n = 12 MCMV: n = 10, MCMVΔIE1: n = 10, Dunn's multiple comparison test $^{*}p < 0.05$; Kruskal–Wallis test: $p = 0.027$). BrdU, bromodeoxyuridine; IE1, immediate early 1; NPC, neural progenitor cell.

Given that patients with congenital CMV infection often display various intellectual deficits depending on the severity of cortical lesions (43), we looked for nonspecific cognitive tests relevant to various cortical dysfunctions. The rodent studies using the lesion of various cortical areas have shown impaired object recognition memory measured by the novel object recognition test (NORT) (44–47). Therefore, we employed NORT to test whether a wide range of brain pathology, including the cortical pathology, was elicited by CMV infection during embryonic development. In P-inj model at postnatal day 84 (3 months of age, 3M), without differing locomotor activity, significant deficits in the NORT were observed when compared with control mice (Fig. 2, *B* and *C*). Consistent observations were also observed in V-inj model at the behavioral levels (Fig. S2, *B* and *C*). Intriguingly, mice infected with mutant MCMV that lacked IE1 (MCMVΔIE1) did not show cognitive deficits, compared with controls at the significant level (Fig. 2*C*).

CMV-encoded IE1 protein perturbs NPC proliferation, which is ameliorated by CRISPR/Cas9 targeting selective to CMV-encoded IE1

During evolution, many pathogens develop strategies that not only enable them to survive under host conditions but also allow them to perturb the host machinery (48). For example, human papilloma virus E6 and E7 proteins interact with host p53 and RB proteins, which lead to the disturbance of the host cell signaling cascade resulting in cervical cancer (49–52). Our experimental data that mice infected with MCMVΔIE1 exhibited no cognitive impairment may suggest that MCMV-encoded IE1 protein may interfere with a host signaling cascade, which may result in CMV infection–elicited cellular pathology in the NPCs and behavioral deficits shown above (Figs. 1 and 2). To address this hypothesis, we ectopically overexpressed MCMV IE1 in the VZ by *in utero* gene transfer and assessed NPC proliferation. We observed a marked reduction in NPC proliferation, as indicated by BrdU labeling

in the VZ/SVZ (Fig. 3*A*). However, introduction of mutant IE1 (IE1Δ135–141) that lacks the domain required for disruption of promyelocytic leukemia (PML) nuclear bodies (53, 54) did not affect NPC proliferation (Fig. 3*A*). These results indicate the pivotal role of MCMV-encoded IE1 in the NPC proliferation in the developing cortex, supporting the idea that viral IE1 and host PML protein interaction may be important for the pathological process.

Thus, we hypothesized that targeting CMV-encoded IE1 based on the CRISPR/Cas9 system (55) and investigating the impact of the NPC pathology may provide further evidence to this notion. We introduced an all-in-one CRISPR/Cas9 vector that can express both Cas9 and the single guide RNA targeting MCMV IE1 gene. We designed target sequences by using two different web-based tools (http://chopchop.cbu.uib.no/, https://www.benchling.com/crispr/) to minimize the off-target effect, and then confirmed the successful targeting by the genome cleavage assay in MCMV-infected cells (Fig. S3). The impact of IE1-CRISPR on the IE1 protein was confirmed by immunostaining for IE1 protein, in which the signal was significantly decreased in MCMV-infected cells cotransfected with IE1-CRISPR compared to MCMV-infected cells cotransfected with the control vector (Fig. 3*B*).

Then, we delivered the most potent IE1-CRISPR construct (the construct #4) into the mouse fetal brain to determine its therapeutic potential for the cellular pathologies caused by congenital CMV infection. Here, we used V-inj model, because the density of IE1-positive cells in P-inj model is relatively sparse, being not optimal to establish the assay condition. Two days after infection/electroporation of MCMV and the IE1-CRISPR vector into the fetal lateral ventricle, the expression level of IE1 protein was significantly decreased in brains with the IE1-CRISPR construct compared to brains with a scrambled-CRISPR construct (Fig. 3*C*). Consequently, the NPC proliferation deficits in MCMV-infected brains were specifically rescued by IE1-CRISPR but not by scrambled-CRISPR (Fig. 3*D*). Taken together, our approach shows that viral IE1-targeting CRISPR delivered *in utero* diminishes MCMV-derived IE1 protein and ameliorates the NPC cellular pathology.

CMV-encoded IE1 protein interferes with the host protein interaction between PML and DISC1, resulting in NPC proliferation deficits

PML is known to function as a front-line defense against viral infection in the nuclear body (56, 57) and, reportedly, interacts with IE1 (58–60). Furthermore, in the neurodevelopmental context, DISC1 protein critically implicated in brain development and NPC proliferation is known to colocalize with the PML nuclear body (61, 62). Thus, we tested a hypothesis to see whether IE1 interferes with the DISC1–PML protein interaction. The hypothesis was experimentally validated: ectopic expression of WT HCMV IE1 almost completely ablates DISC1-PML binding in human cells, whereas mutant HCMV IE1-L174P, which is reportedly defective in binding with PML (58–60), failed to block the DISC1-PML protein binding (Fig. 4*A*).

In parallel, we generated an expression construct of human PML lacking the IE1-binding site (281–304 amino acid residues) (PMLΔIE1) (63, 64). This mutant PML retained the interaction with DISC1, and the DISC1–PML interaction was not affected by IE1 (Fig. 4*B*). Consistent with these observations, infection of HCMV perturbed DISC1-PML colocalization in human cells (Fig. S4*A*).

To prove that the interference of DISC1-PML binding by viral IE1 is critically relevant to CMV-elicited NPC pathology, the significance of the protein binding in proper NPC proliferation *in vivo* was investigated. We first looked for amino acid residues that are required for the binding of DISC1 with PML using established peptide array and coimmunoprecipitation approaches (65). This investigation resulted in identifying the residues 147 to 150 of DISC1 (Figs. 4*C* and S4*B*) and generating the mutant deficient of these four amino acid residues (DISC1ΔPML). As shown in previous publications (66, 67), *in utero* knockdown of DISC1 leads to NPC proliferation deficits in the developing cortex, which are rescued with coexpression of WT DISC1. However, we failed to observe the rescue by coexpression of DISC1ΔPML (Fig. 4*D*). This suggests that DISC1-PML binding, which is disrupted by CMV-encoded IE1, is required for proper NPC proliferation during development.

Disturbance of Notch pathway in CMV-infected NPC: a downstream of perturbed PML–DISC1 interaction

DISC1 is known to regulate NPC proliferation, at least through the Wnt pathway (66, 67). Thus, we first tested whether loss of the DISC1–PML protein interaction might affect the Wnt pathway by using β-catenin transcriptional activity as the readout in an established reporter system, in which Renilla luciferase was used as an internal control (66). As published by multiple groups (66–68), knockdown of DISC1 by RNAi at E13.5 induced a significant reduction of Wnt/β-catenin signaling activity at E15.5 with its full rescue by WT DISC1 (Figs. 5*A* and Table S1*A*). However, the effect of DISC1ΔPML was unique: although DISC1ΔPML was completely unable to rescue NPC proliferation deficits elicited by DISC1 knockdown (Fig. 4*D*), DISC1ΔPML could partially, but not fully rescue the deficits in the Wnt pathway (Fig. 5*A*, and Table S1*A*). One possible scenario to account for these data is that DISC1 is involved in NPC proliferation through not only the Wnt pathway but also another cascade, for both of which DISC1–PML interaction is required. *In vitro* infection study indicates that CMV dysregulates Notch pathway which may alter differentiation and proliferation in NPCs (69, 70). Thus, we hypothesized the possible involvement of the Notch pathway as the primary target. We tested this idea by using an established C-promoter binding factor 1 (CBF1) reporter system (71), in which Renilla luciferase was used as an internal control (66). Knockdown of DISC1 suppressed Notch/CBF1 activity, which was rescued by WT DISC1, but not by the DISC1ΔPML mutant (Fig. 5*B* and Table S1*B*). This suggests that the DISC1–PML interaction is necessary for the Notch signaling in the developing cortex. Altogether, it is

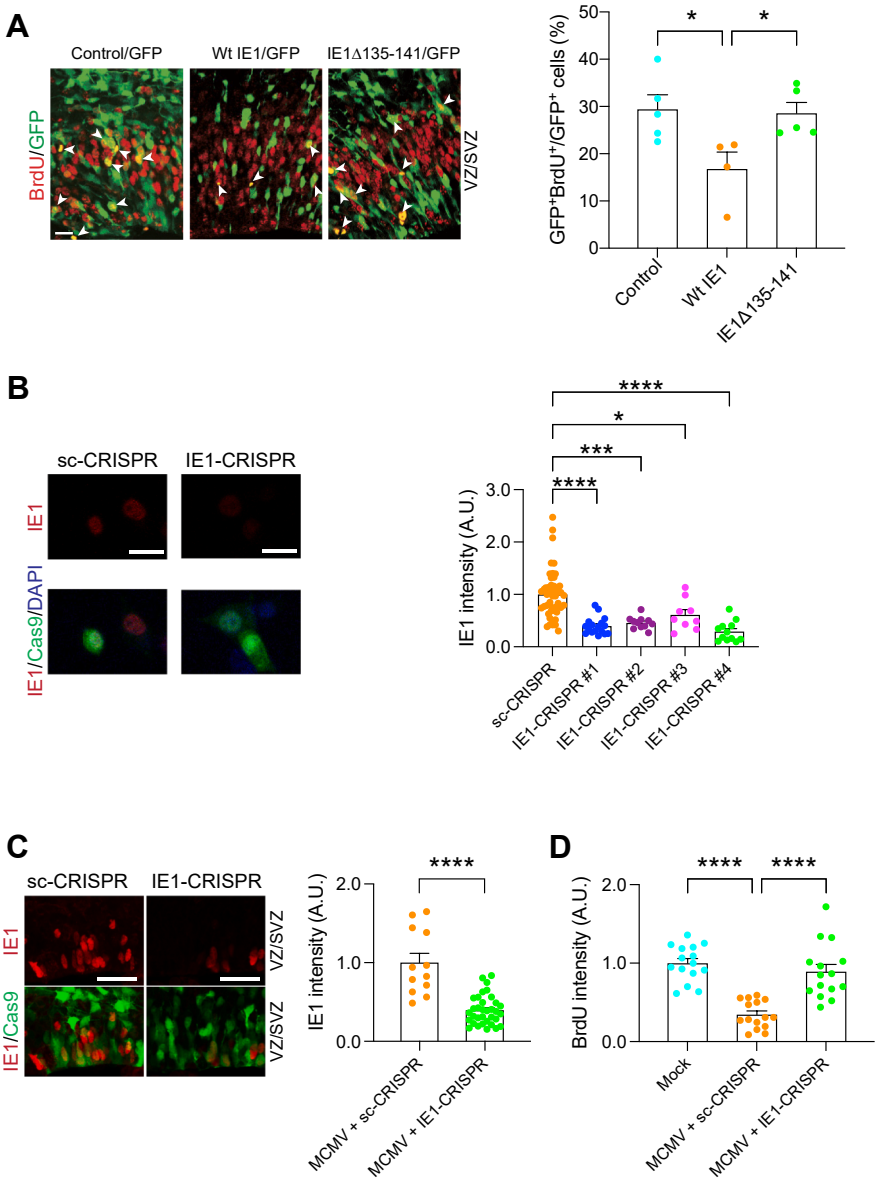

Figure 3. IE1-targeting CRISPR delivery *via in utero* depletes viral IE1, and rescues the brain pathologies. *A,* mouse embryos electroporated with control, WT or mutant IE1 plasmid, and a GFP construct at E13.5 were pulse labeled with BrdU at E15.5. *Green*, cells transfected with GFP and control or IE1; *red*, BrdU-positive cells; *arrowheads*, GFP- and BrdU-double positive cells. The scale bar represents 20 μm. Bar graph represents the percentage of GFP- and BrdU-double positive cells over total GFP-positive cells in the VZ/SVZ. Graph shows mean +/− s.e.m. (Control: n = 5, WtIE1: n = 4, IE1Δ135–141: n = 11, Tukey's multiple comparison test *$p < 0.05$; one-way ANOVA: F(2,11) = 5.246, $p = 0.025$). *B,* HT-22 cells were transfected with IE1-CRISPR (target #1–#4) or sc-CRISPR (control) plasmids. Twenty-four hours after transfection, MCMV was infected to the cells. Then, 24 h after infection, immunoreactivity for IE1 (*red*) was assessed. Graph indicates the expression level of IE1 protein in Cas9-positive cells among four candidates of IE1 target sequences and control. *Red*, IE1; *green*, Cas9; *blue*, DAPI. The scale bar represents 25 μm. Graph shows mean +/− SEM (sc-CRISPR: n = 49, IE1-CRISPR#1: n = 17, IE1-CRISPR#2: n = 11, IE1-CRISPR#3: n = 9, IE1-CRISPR#4: n = 12, Dunn's multiple comparison test *$p < 0.05$, ***$p < 0.001$, and ****$p < 0.0001$; Kruskal–Wallis test: $p < 0.0001$). *C,* E14.5 embryonic brains were electroporated with IE1-CRISPR or sc-CRISPR plasmids and analyzed at E16.5. The graph indicates expression level of IE1 protein in cells transfected with IE1/or sc-CRISPR. *Red*, IE1; *green*, Cas9; the scale bar represents 25 μm. Graph shows mean +/− SEM (MCMV + sc-CRISPR: n = 12, MCMV + IE1-CRISPR: n = 34, ****$p < 0.0001$; two-tailed Student's *t* test). *D,* MCMV-infected mouse embryos electroporated with sc- or IE1-CRISPR at E14.5, and mock-injected mice pulse labeled with BrdU at E16.5. The graph represents the intensity level of BrdU in IE1 and Cas9-double positive cells or cells from mock-injected mice in the ventricular zone/subventricular zone (VZ/SVZ). Graph shows mean +/− SEM (n = 15 per group, Tukey's multiple comparison test ***$p < 0.001$, ****$p < 0.0001$; one-way ANOVA: F(2,42) = 26.73, $p < 0.0001$). DAPI, 4′,6-diamidino-2-phenylindole; PML, promyelocytic leukemia; E16.5, embryonic day 16.5; E15.5, embryonic day 15.5; BrdU, bromodeoxyuridine.

likely that MCMV infection and the viral-derived IE1 protein may disturb the host DISC1–PML protein interaction, which in turn affects cellular signaling including the Notch pathway. Consistent with this notion, we observed a significant reduction in the immunoreactivity of HES1, a key transcription factor activated by Notch signaling in IE1-positive (MCMV-infected) cells compared to IE1-negative cells (Fig. 5*C*).

Discussion

In the present study, we deciphered an intracellular molecular mechanism that can account for the deficits of NPC

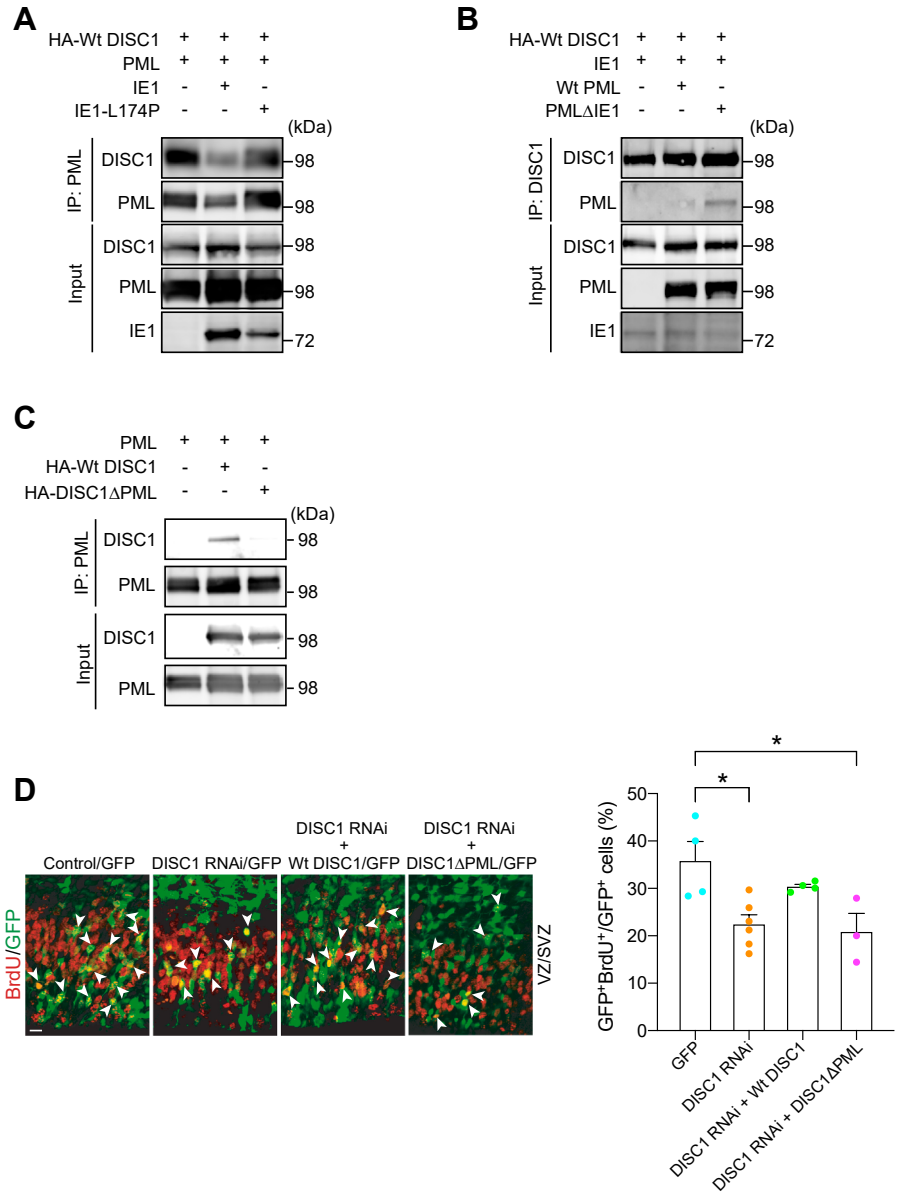

Figure 4. DISC1–PML interaction is required for NPC proliferation in the developing cortex. *A,* lysates from human embryonic kidney (HEK) cells co-transfected with DISC1, PML and WT IE1 or IE1-L174P were immunoprecipitated with an anti-PML antibody and immunoblotted with an anti-HA antibody. *B,* lysates from HEK cells cotransfected with DISC1, IE1, and WT PML or mutant PML lacking the IE1-binding site (PMLΔIE1) were immunoprecipitated with an anti-PML antibody and immunoblotted with an anti-HA antibody. *C,* HEK cells cotransfected with PML and HA-tagged WT DISC1, or mutant DISC1 lacking the PML-binding site (DISC1ΔPML), were immunoprecipitated with the PML antibody and immunoblotted with the HA antibody. *D,* mouse embryos electroporated with various constructs at E13.5 were pulse labeled with BrdU (50 mg/kg) for 2 h at E15.5. *Bar graph* represents the percentage of GFP- and BrdU-double positive cells over total GFP-positive cells in the VZ/SVZ. *Green*, cells transfected with GFP, DISC1 RNAi, and DISC1 constructs; *red*, BrdU-positive cells; *arrowheads* indicate GFP- and BrdU-double positive cells. The scale bar represents 20 μm. Graph shows mean +/− SEM (GFP: n = 4, DISC1 RNAi: n = 6, DISC1 RNAi + Wt DISC1: n = 4, DISC1 RNAi + DISC1ΔPML: n = 3, Tukey's multiple comparison test *$p < 0.05$; one-way ANOVA: $F(3,13) = 6.067$, $p = 0.0082$). BrdU, bromodeoxyuridine; E13.5, embryonic day 13.5; E15.5, embryonic day 15.5; HA, hemagglutinin; NPC, neural progenitor cell; IE1, immediate early 1; SZ, subventricular zone; VZ, ventricular zone; PML, promyelocytic leukemia.

proliferation in congenital CMV infection. We demonstrated that delivering IE1-targeting CRISPR/Cas9 to the fetal brain inhibits production of the viral IE1 protein and rescues the NPC pathology in the mouse model. The present study allows us to gain insight into a mechanism in the host pathophysiology of congenital CMV infection.

The success of modeling in C57BL/6 mice here, in contrast to many past studies that tended to use different strains to avoid the potential risk of C57BL/6-associated genetic resistance to the viral infection (25, 34, 35), will facilitate well-standardized behavioral assays and the utilization of many genetic tools available in the C57BL/6 strain for in-depth mechanistic study. Specifically, in the present study, we uncover a mechanism for how a specific viral protein affects biological systems in the host and elicits critical pathology, which was facilitated by leveraging the delivery of the CRISPR/Cas9 system. The rapid progress of medical technology for genome editing and delivery system has provided hope for a novel therapeutic strategy based on mechanism-guided target(s). Thus, we hope that the approach employed

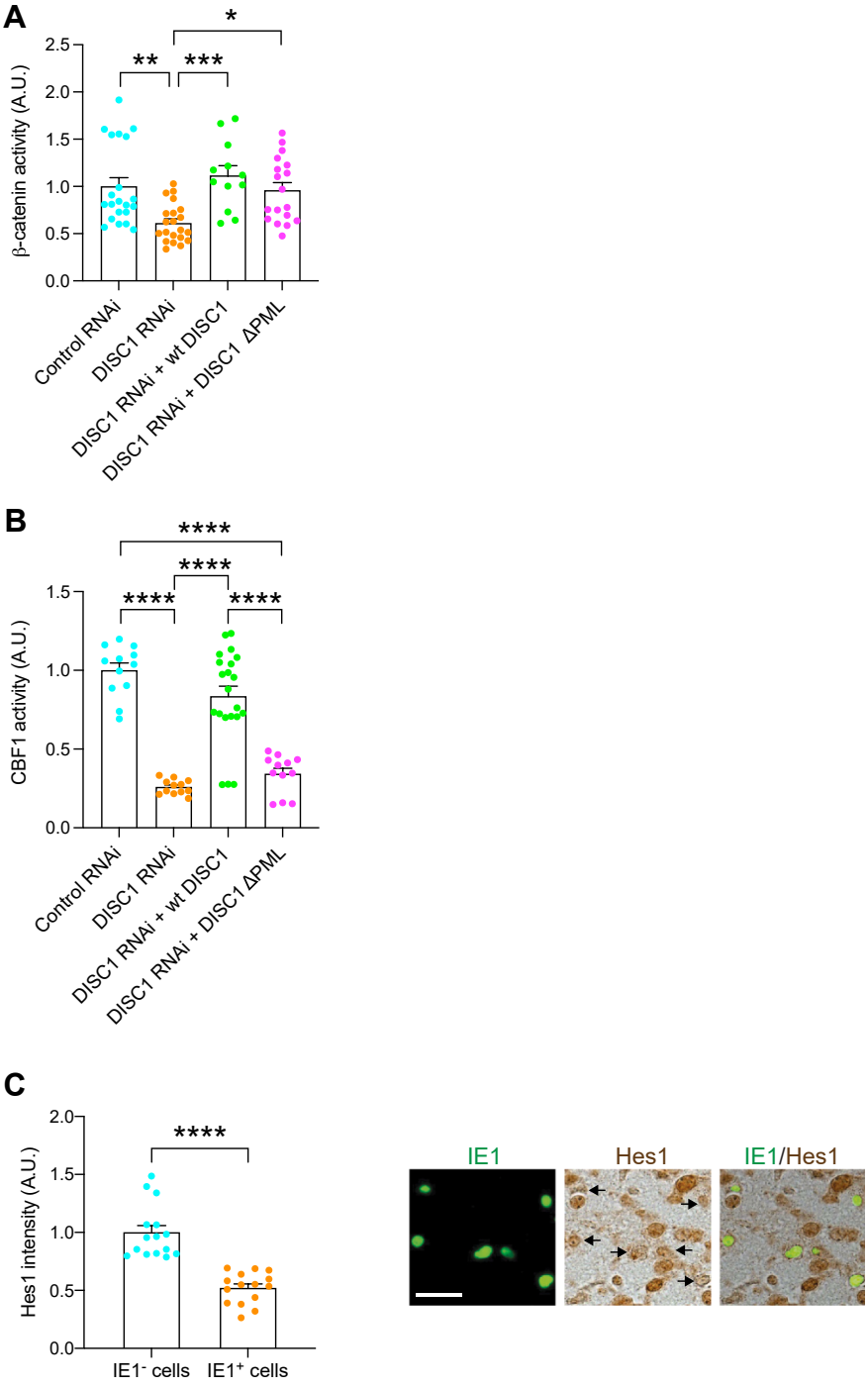

Figure 5. DISC1-PML protein is involved in NPC proliferation *via* the Notch pathway. *A,* Super8XTOPFlash and pRL SV40 plasmids together with various constructs were injected into the lateral ventricles *in utero* at E13.5 and analyzed at E15.5. Knockdown of DISC1 suppressed β-catenin–dependent activity, which was fully rescued by WT DISC1 and partially rescued by DISC1ΔPML. Graph shows mean +/− SEM (Control RNAi: n = 21, DISC1 RNAi: n = 21, DISC1 RNAi + Wt DISC1: n = 12, DISC1 RNAi + DISC1ΔPML: n = 18, Dunn's multiple comparison test *$p < 0.05$, **$p < 0.01$, ***$p < 0.001$; Kruskal–Wallis test: $p < 0.0001$). *B,* reporter plasmids containing a CBF1-responsive element along with various constructs were injected into the lateral ventricles *in utero* at E13.5 and analyzed at E15.5. Graph shows CBF1 activity between groups and mean ± SEM (Control RNAi: n = 12, DISC1 RNAi: n = 12, DISC1 RNAi + Wt DISC1: n = 21, DISC1 RNAi + DISC1ΔPML: n = 12, Tukey's multiple comparison test ***$p < 0.001$; one-way ANOVA: F(3,53) = 41.58, $p < 0.0001$). *C,* MCMV-infected brains were immunostained with IE1 (*green*) and Hes1 (*brown*); the scale bar represents 25 μm. Graph indicates the expression level of Hes1 in the IE1-positive or negative cells. Graph shows mean +/− SEM (n = 15 per group, ****$p < 0.0001$; two-tailed Student's *t* test). CBF1, C-promoter binding factor 1; E13.5, embryonic day 13.5; E15.5, embryonic day 15.5; NPC, neural progenitor cell; IE1, immediate early 1; PML, promyelocytic leukemia.

here may have a chance to open a new therapy of congenital CMV infection.

Given that the deficit of NPC proliferation is a key pathological event for congenital CMV infection, this question has been addressed by other groups (72, 73). For example, there is a report indicating that HCMV activates PPARγ in neural stem cells from human embryonic stem cells and brain sections from infected fetuses (72). Both PML and PPARγ are

nuclear proteins, and functional cross-talks of these molecules have been reported (74). Whether and how the PML-DISC1 and PPARγ cascades interact will be an interesting question in the future.

We acknowledge that the present study provides many more questions that are to be addressed in future studies. First, although other rodent models may show a wider range of behavioral changes (23, 25, 75), the present models show more specific changes. This may be affected by the difference of mouse strains. We regard these differences as an opportunity of exploring the link between the neuropathology and behavioral changes by comparing different rodent models. In this case, we believe that this study providing new rodent models will be meaningful for the overall study of congenital CMV infection. Second, there is a question of whether the host–viral protein interaction is only limited to NPCs or all other CMV-infected cells. Given that DISC1 is almost predominantly expressed in NPCs and early-stage differentiated neurons, this mechanism may play a role more prominently in NPCs. Finally, the significance of IE1 will be further validated by using MCMV-expressing mutant IE1 (*e.g.*, IE1Δ135-141).

Experimental procedures

Reagents and chemicals

Constructs

We used the RNAi constructs to mouse and human DISC1 that have been established in previous publications from other groups and ours (40, 66, 67). Glutathione-*S*-transferase (GST)-tagged human PML IV and FLAG-tagged human PML IV deletion constructs were a generous gift from Dr Pandolfi (Beth Israel Deaconess Cancer Center). Human IE1 expression constructs, hemagglutinin (HA) and FLAG-tagged human PML VI, were obtained from Dr Hayward (Johns Hopkins University). Plasmid pp89 expressing MCMV IE1 expression constructs as well as mutant MCMV IE1 (IE1 with deletion of amino acids residues 135–141, IE1Δ135–141) were kindly provided by Dr Gerd Maul (Wistar Institute). Human PML I (hPML) expression construct (GenScript: OHu25455) was used for a generation of mutant hPML [hPML with deletion of IE1-binding site (amino acid residues 281–304), PMLΔIE1] expression construct. The following primers were used: forward, 5′-GATCCGCTACCAGCGCGACTACGAG-3′; reverse, 5′-CGCTGGTAGCGGATCAGCTCCTCGG-3′. Target sequences in MCMV IE1 (MCMV, GenBank #U68299) were determined using the CRISPR design tool from the http://crispr.mit.edu/(Zhang lab, MIT) and http://chopchop.cbu.uib.no (Harvard University) websites. The target oligos (Table S2) were inserted into the plasmid that was purchased from Addgene (pCAG-eCas9-GFP-U6-gRNA, #79145) using a restriction enzyme (BbsI) digestion and ligation approach and transformed into SURE2 competent cells (Agilent Technologies).

Viruses

MCMV-Smith strain and IE1(exon4)-deleted MCMV (MCMVΔIE1) and IE1(exon4)-deleted HCMV (CMVΔIE1) and the parent WT HCMV-Towne strain were reported previously (63, 76).

Antibodies

For immunofluorescence and immunoblotting, HA-tagged proteins were detected with a rat monoclonal anti-HA antibody (ROCHE) or a mouse monoclonal anti-HA antibody (Covance). Flag-tagged proteins were detected with a polyclonal antibody against FLAG (Sigma). The following antibodies were also used: mouse monoclonal anti-human PML (Santa Cruz); mouse monoclonal anti-mouse PML (Chemicon, Millipore); mouse monoclonal anti-IE1 (kindly provided by Dr Qiyi Tang, Howard University) (25); rat anti-BrdU (Chemicon). The customized antibodies against mouse DISC1 (77) and human DISC1 (23, 62) were used to detect endogenous DISC1.

Recombinant proteins tagged with GST or maltose-binding protein)

Full-length mouse DISC1 cDNA was cloned in a pMAL vector for DISC1-maltose-binding protein. The expression plasmids were introduced into *Escherichia coli* (*E. coli*) BL21, grown at 23 °C with 0.1 mM IPTG. Recombinant proteins were purified from *E. coli* with glutathione sepharose or amylase beads.

Cells

SK-N-MC human neuroblastoma cells and HEK cells were purchased from ATCC. SK-N-MC cells were grown in Dulbecco's modified Eagle's medium (DMEM)/F-12 with 10% fetal bovine serum. HT-22 (66) and HEK cells were grown in DMEM with 10% fetal bovine serum. SK-N-MC, HT-22, and HEK cells were transfected with lipofectamine 2000 (Invitrogen). SK-N-MC human neuroblastoma cells were seeded on round coverslips in 24-well plates and infected with either CMVΔIE1 or the parent Towne virus for 24 h. *Mycoplasma* testing is carried out in Johns Hopkins Genetic Resources Core Facility.

Biochemical and cellular assays

SPOT-synthesis of peptides and overlay experiments—Peptide libraries were produced by automatic SPOT-synthesis. Peptides were synthesized on continuous cellulose membrane supports on Whatman 50 cellulose membranes by using Fmoc (9-fluoromethyloxycarbonyl) chemistry with the Autobot Spot-Robot ASS 222 (Intavis Bioanalytical Instruments) (78). Interaction of peptide spots with purified recombinant GST- or GST-PML (human PML IV) fusion protein was determined by overlaying the cellulose membranes with 10 mg/ml of recombinant protein. Bound recombinant proteins were detected with anti-GST antisera (Santa Cruz Biotechnologies) and a complementary horseradish peroxidase-coupled secondary antibody for immunoblotting.

Immunoprecipitation—Cells or tissues were lysed in lysis buffer (150 mM NaCl, 50 mM Tris–HCl, pH 7.5, 1% Triton X-100) containing a protease inhibitor mixture (Roche

Applied Sciences). Lysates were sonicated, cell debris was cleared by centrifugation, and the soluble fraction was immunoprecipitated as described previously (40, 66). Western blotting images were developed by immunofluorescence and captured by Amersham Typhoon biomolecular imagers (Cytiva). The captured images were quantified by densitometric analyses using ImageJ software (https://imagej.net/ij/).

Immunocytochemistry—Cells were seeded on round coverslips (Corning Glass Inc) in 24-well plates (Falcon; Becton Dickinson Labware), washed once with PBS, and fixed in ice cold methanol at −20 °C for 15 min. The cells were then washed three times in PBS and blocked in 10% bovine serum albumin for 30 min at room temperature. Cells were incubated with the primary antibody at 4 °C overnight. After 24 h, cells were washed three times in PBS before addition of a secondary antibody conjugated with Rhodamine X (red), Cy2 or Alexa 488 (green), Cy5 (white) of either anti-rabbit, anti-rat, or anti-mouse IgG for 45 min at room temperature. After a final wash with PBS, cells were stained with 4′,6-diamidino-2-phenylindole.

In vitro *genome cleavage assay*—HT-22 cells were transfected with an IE1-targeting CRISPR/Cas9 plasmid or control plasmid and cultured at 37 °C. Twenty-four hours after transfection, cells were infected with MCMV. Twenty-four hours after MCMV infection, cells were collected, and genomic DNA was isolated with the DNeasy Blood and Tissue Kit (QIAGEN). The region including the target sites was PCR-amplified using the primers described in Table S3. The PCR products were denatured and re-annealed using a thermal cycler. The heteroduplex DNA containing the insertion, deletion, or mismatched DNA (indel) was cleaved by T7 endonuclease 1. Gel analysis was performed to detect the cleaved DNA fragments.

Animal studies—Modeling and histological analyses—all experiments were performed in accordance with protocols approved by the Animal Care and Use Committees of Johns Hopkins University and Hamamatsu University School of Medicine. The C57BL/6 male and female mice were purchased from Jackson Laboratory and used for timed-mating. These C57BL/6 mice were used for viral infection and *in utero* electroporation (see below).

Intraplacental MCMV injection (P-inj)—MCMV (Smith strain) was prepared and the titer of viral stock was determined as described previously. The dose of MCMV and the time of intraplacental infection and euthanization were first determined so that sufficient survival of MCMV-infected fetuses (>80%) and adequate viral infection and BrdU incorporation in fetal brains were established. At E14.5 pregnant mice were anaesthetized by an intraperitoneal injection of 0.2 to 0.3 ml of 10% Somnopentyl and uterine horns were exposed. With use of glass micropipettes, 1×10^5 plaque-forming units of MCMV in 1 μl of DMEM were injected through the uterine wall into the labyrinth region in half of the placentas. Mock-infected placentas were injected with DMEM. Two days (E16.5) after infection, BrdU (50 mg/kg) was injected intraperitoneally into pregnant mice. Three hours later, fetal brains were fixed by perfusion with 4% paraformaldehyde, immersed in 25% sucrose, and frozen in liquid nitrogen. Coronal sections were serially cut with a cryostat at 12 μm. Those days (E14.5–16.5) correspond to Carnegie Stages 20 to 23, late first-trimester of pregnancy in humans, are critical to brain development.

Ventricular MCMV injection (V-inj)—General *in utero* surgery was as described above. E14.5 pregnant mice were anesthetized, and uterine horns were exposed. With use of glass micropipettes, 1×10^5 plaque-forming unit of MCMV in 1 μl of DMEM were injected through the uterine wall into the lateral ventricle of embryos. Mock-infected fetuses were injected with DMEM into the lateral ventricle.

In utero *electroporation*—Pregnant C57BL/6 mice at E13.5 or E14.5 were deeply anesthetized by intraperitoneal administration of a mixed solution of Ketamine HCl (100 mg/kg) and Xylazine HCl (7.5 mg/kg), and intrauterine embryos were surgically manipulated as described previously (40, 79) with slight modifications. Plasmid solutions (1–2 μl) containing DISC1 RNAi plasmids (2 μg/μl) together with a CMV early enhancer/chicken β-actin promoter-driven GFP expression vector (1 μg/μl) were injected into the lateral ventricles. For the rescue experiments, a combination of a DISC1 RNAi plasmid (2 μg/μl in 1 μl) with a WT or mutant (DISC1ΔPML) DISC1 expression plasmid (1 μg/μl in 1 μl) together with a CMV early enhancer/chicken β-actin promoter-driven GFP expression vector (1 μg/μl in 1 μl) were injected. To use the same amount of DNA for each condition, an empty expression vector (pCAGGS1) was used as necessary. To perform rescue experiments in the intraplacental MCMV infection mice, an IE1-targeting CRISPR expression plasmid (1.5 μg/μl in 1 μl) together with a CMV early enhancer/chicken β-actin promoter-driven GFP expression vector (1 μg/μl in 1 μl) were injected into the lateral ventricles when the embryos were intraplacentally infected with MCMV. Electrical pulses (35 V, 50 ms, 4 times) were applied using an electroporator (CUY21E, Tokiwa Science) with a forceps-type electrode (CUY650-5, Tokiwa Science).

Brain slice preparation, immunohistochemistry, and BrdU incorporation assay—Histological procedures were performed as previously described with minor modifications (66). Brains were fixed with 4% paraformaldehyde, and coronal sections were obtained with a cryostat at 20 μm (CM 1850, Leica) at E16.5. For immunohistochemistry, the following primary antibodies were used: anti-BrdU (1:500) and anti-HA and anti-GFP (1:500). Fluorescent secondary antibodies conjugated to Alexa 488, Alexa 568, and Alexa 594 (Molecular Probes) were used. Nuclei were labeled with 4′,6-diamidino-2-phenylindole (DAPI) (Molecular Probes). Images of the slices were acquired with a confocal microscope (LSM 700, Zeiss). For BrdU incorporation assay, BrdU (50 mg/kg) was injected i.p. into pregnant mice 2 days after electroporation. Embryonic brains were extracted 2 h after BrdU injection. The cryosections were incubated in PBS with 0.01% Triton X100 for 30 min, and then 1 N HCl at 37 °C for 30 min. After washing with PBS, the sections were

immunostained with a rat anti-BrdU antibody (Chemicon). Optical density of immunoreactivity in Western blotting was obtained with ImageJ software. Number of the IE1-positive cells was counted by the Volocity Software (https://www.volocity4d.com/) (ParkinElmer).

β-Catenin and CBF1 activity assays with luciferase reporter system—Luciferase reporter system assays were carried out by using either the β-catenin or CBF1 reporter plasmid together with pRL-SV40 plasmid (Renilla luciferase, internal control) (66). Expression and/or RNAi constructs, as well as reporter plasmids, were delivered into the VZ at E13.5 by *in utero* electroporation. The luciferase activity was measured at E15.5 (66).

Behavioral assays—Only male mice were used for the behavioral assays to avoid confounding effects from the female estrous cycle. Open field test was conducted as described previously (80) with minor modifications. In brief, each mouse was placed in a transparent acrylic cage (40 cm × 40 cm; San Diego Instruments) for 30 min. Locomotor activities were recorded by an infrared activity monitor (San Diego Instruments). A single beam break was reported as "count." For novel object recognition test, mice were habituated to the testing box over 3 days. On day 4, the mice were exposed to two objects for 10 min. On day 5 (retention), one familiar object was replaced with a novel object and the mice were allowed to explore both objects for 5 min. The preference index was calculated as the ratio of time spent exploring the novel object in the retention session to total exploration time.

Statistical analyses

All statistical analyses were performed using GraphPad Prism 10 (https://www.graphpad.com/). Data normality was assessed using the Shapiro–Wilk or Kolmogorov–Smirnov test. If all groups passed the normality test, the two-tailed Student's t test was used for comparisons between two independent groups, with statistical significance defined as $p < 0.05$. For comparisons involving more than two groups, one-way ANOVA was performed followed by Tukey's multiple comparison test; results were considered significant at $p < 0.05$. If any group failed the normality test, the Mann–Whitney test was used for comparisons between two independent groups, with significance defined as $p < 0.05$. For comparisons involving more than two groups under nonparametric conditions, Kruskal–Wallis test was performed followed by Dunn's multiple comparison test; results were considered significant at $p < 0.05$.

Data availability

All data generated or analyzed during this study are included in this article and its supplementary information files.

Supporting information—This article contains supporting information.

Acknowledgments—We thank Ms Ruth Cruz for virus preparation, Ms Y. Lema for preparing the figures and organizing the manuscript, and Dr M. Salgado, Dr P. Talalay, and Ms L. Guttman for critical reading of this manuscript.

Author contributions—A. Saito, K. Ishizuka, and A. Sawa writing–original draft; A. Saito, S. T., K. Ishii, K. Ishizuka, and A. Sawa methodology; A. Saito, S. T., K. Ishii, M. S.-S., E. C. O., H. M., S. A., K. F., M. F., R. H. Y., M. D. H., N. K., I. K., A. K., and K. Ishizuka investigation; P. S., G. G. M., G. S. H., and Q. T. resources; K. Y. formal analysis; A. Sawa supervision; A. Sawa project administration; A. Sawa funding acquisition; A. Sawa conceptualization.

Funding and additional information—This work was supported by USPHS grants MH136297 Silvio O. Conte center (A. Sawa, A. K, and K. Y.), MH094268 Silvio O. Conte center (A. Sawa, N. K., and A. K.), MH105660 (A. Sawa and K. Ishizuka), MH091230 (A. K.), MH96208 (K. Ishizuka), SC1AI112785 (Q. T.) as well as foundation grants from the Stanley Foundation (A. Sawa), RUSK/S&R Foundation (A. Sawa), Brain & Behavior Research Foundation (A. Saito, E. C. O, K. Ishizuka, A. K., and A. Sawa), Japan Health Sciences Foundation (SHC4401; I. K.), and Subsidies for Current Expenditures to Private Institutions of Higher Education from the Promotion and Mutual Aid Corporation for Private Schools of Japan (K. Ishizuka).

Conflict of interest—A. Sawa reports a relationship with American Association for the Advancement of Science that includes board membership. A. Sawa reports a relationship with Sumitomo Pharma Co Ltd that includes consulting or advisory. The other authors declare that they have no conflicts of interest with the contents of this article.

Abbreviations—The abbreviations used are: BrdU, bromodeoxyuridine; CBF1, C-promoter binding factor 1; CMV, cytomegalovirus; DMEM, Dulbecco's modified Eagle's medium; E14.5, embryonic day 14.5; GST, glutathione-*S*-transferase; HCMV, human CMV; hPML, human PML I; IE1, immediate early 1; NPC, neural progenitor cell; P-inj model, intraplacental injection model; PML, promyelocytic leukemia; SZ, subventricular zone; V-inj, ventricular injection model; VZ, ventricular zone.

References

1. Cannon, M. J. (2009) Congenital Cytomegalovirus (CMV) epidemiology and awareness. *J. Clin. Virol.* **46**, S6–S10
2. Kenneson, A., and Cannon, M. J. (2007) Review and meta-analysis of the epidemiology of congenital Cytomegalovirus (CMV) infection. *Rev. Med. Virol.* **17**, 253–276
3. Weller, T. H. (1971) The cytomegaloviruses: ubiquitous agents with protean clinical manifestations. I. *N. Engl. J. Med.* **285**, 203–214
4. Ivarsson, S. A., Lernmark, B., and Svanberg, L. (1997) Ten-year clinical, developmental, and intellectual follow-up of children with congenital cytomegalovirus infection without neurologic symptoms at one year of age. *Pediatrics* **99**, 800–803
5. Cheeran, M. C., Lokensgard, J. R., and Schleiss, M. R. (2009) Neuropathogenesis of congenital cytomegalovirus infection: disease mechanisms and prospects for intervention. *Clin. Microbiol. Rev.* **22**, 99–126
6. Murray, C. J., Vos, T., Lozano, R., Naghavi, M., Flaxman, A. D., Michaud, C., *et al.* (2012) Disability-adjusted life years (DALYs) for 291 diseases and injuries in 21 regions, 1990-2010: a systematic analysis for the Global Burden of Disease Study 2010. *Lancet* **380**, 2197–2223

7. Cannon, M. J., Schmid, D. S., and Hyde, T. B. (2010) Review of cytomegalovirus seroprevalence and demographic characteristics associated with infection. *Rev. Med. Virol.* **20**, 202–213
8. van der Sande, M. A., Kaye, S., Miles, D. J., Waight, P., Jeffries, D. J., Ojuola, O. O., *et al.* (2007) Risk factors for and clinical outcome of congenital cytomegalovirus infection in a peri-urban West-African birth cohort. *PLoS One* **2**, e492
9. Duryea, E. L., Sanchez, P. J., Sheffield, J. S., Jackson, G. L., Wendel, G. D., McElwee, B. S., *et al.* (2010) Maternal human immunodeficiency virus infection and congenital transmission of cytomegalovirus. *Pediatr. Infect. Dis. J.* **29**, 915–918
10. Frederick, T., Homans, J., Spencer, L., Kramer, F., Stek, A., Operskalski, E., *et al.* (2012) The effect of prenatal highly active antiretroviral therapy on the transmission of congenital and perinatal/early postnatal cytomegalovirus among HIV-infected and HIV-exposed infants. *Clin. Infect. Dis.* **55**, 877–884
11. Kovacs, A., Schluchter, M., Easley, K., Demmler, G., Shearer, W., La Russa, P., *et al.* (1999) Cytomegalovirus infection and HIV-1 disease progression in infants born to HIV-1-infected women. Pediatric Pulmonary and Cardiovascular Complications of Vertically Transmitted HIV Infection Study Group. *N. Engl. J. Med.* **341**, 77–84
12. Guibert, G., Warszawski, J., Le Chenadec, J., Blanche, S., Benmebarek, Y., Mandelbrot, L., *et al.* (2009) Decreased risk of congenital cytomegalovirus infection in children born to HIV-1-infected mothers in the era of highly active antiretroviral therapy. *Clin. Infect. Dis.* **48**, 1516–1525
13. National Center for Hearing Assessment and Management U.S. (2016) *Journal of Early Hearing Detection and Intervention National Center for Hearing Assessment and Management at*, Utah State University, Logan, UT
14. Nigro, G., Adler, S. P., Parruti, G., Anceschi, M. M., Coclite, E., Pezone, I., *et al.* (2012) Immunoglobulin therapy of fetal cytomegalovirus infection occurring in the first half of pregnancy–a case-control study of the outcome in children. *J. Infect. Dis.* **205**, 215–227
15. Whitley, R. J. (2019) Congenital cytomegalovirus and Neonatal Herpes Simplex virus infections: to treat or not to treat? *Pediatr. Infect. Dis. J.* **38**, S60–S63
16. Schleiss, M. R., Permar, S. R., and Plotkin, S. A. (2017) Progress toward development of a vaccine against Congenital Cytomegalovirus Infection. *Clin. Vaccine Immunol.* **24**, e00268-17
17. Permar, S. R., Schleiss, M. R., and Plotkin, S. A. (2025) A vaccine against cytomegalovirus: how close are we? *J. Clin. Invest.* **135**, e182317
18. Dogra, P., and Sparer, T. E. (2014) What we have learned from animal models of HCMV. *Methods Mol. Biol.* **1119**, 267–288
19. Cekinovic, D., Lisnic, V. J., and Jonjic, S. (2014) Rodent models of congenital Cytomegalovirus infection. *Methods Mol. Biol.* **1119**, 289–310
20. Woolf, N. K., Jaquish, D. V., and Koehrn, F. J. (2007) Transplacental murine cytomegalovirus infection in the brain of SCID mice. *Virol. J.* **4**, 26
21. Li, L., Kosugi, I., Han, G. P., Kawasaki, H., Arai, Y., Takeshita, T., *et al.* (2008) Induction of cytomegalovirus-infected labyrinthitis in newborn mice by lipopolysaccharide: a model for hearing loss in congenital CMV infection. *Lab. Invest.* **88**, 722–730
22. Koontz, T., Bralic, M., Tomac, J., Pernjak-Pugel, E., Bantug, G., Jonjic, S., *et al.* (2008) Altered development of the brain after focal herpesvirus infection of the central nervous system. *J. Exp. Med.* **205**, 423–435
23. Ornaghi, S., Hsieh, L. S., Bordey, A., Vergani, P., Paidas, M. J., and van den Pol, A. N. (2017) Valnoctamide inhibits cytomegalovirus infection in developing brain and attenuates neurobehavioral dysfunctions and brain abnormalities. *J. Neurosci.* **37**, 6877–6893
24. Li, R. Y., and Tsutsui, Y. (2000) Growth retardation and microcephaly induced in mice by placental infection with murine cytomegalovirus. *Teratology* **62**, 79–85
25. Zhou, Y. P., Mei, M. J., Wang, X. Z., Huang, S. N., Chen, L., Zhang, M., *et al.* (2022) A congenital CMV infection model for follow-up studies of neurodevelopmental disorders, neuroimaging abnormalities, and treatment. *JCI Insight* **7**, e152551
26. Moulden, J., Sung, C. Y. W., Brizic, I., Jonjic, S., and Britt, W. (2021) Murine models of central nervous system disease following congenital human cytomegalovirus infections. *Pathogens* **10**, 1062
27. Sakao-Suzuki, M., Kawasaki, H., Akamatsu, T., Meguro, S., Miyajima, H., Iwashita, T., *et al.* (2014) Aberrant fetal macrophage/microglial reactions to cytomegalovirus infection. *Ann. Clin. Transl Neurol.* **1**, 570–588
28. Schleiss, M. R. (2002) Animal models of congenital cytomegalovirus infection: an overview of progress in the characterization of Guinea pig cytomegalovirus (GPCMV). *J. Clin. Virol.* **25**, S37–S49
29. Teissier, N., Fallet-Bianco, C., Delezoide, A. L., Laquerriere, A., Marcorelles, P., Khung-Savatovsky, S., *et al.* (2014) Cytomegalovirus-induced brain malformations in fetuses. *J. Neuropathol. Exp. Neurol.* **73**, 143–158
30. Kosugi, I., Shinmura, Y., Kawasaki, H., Arai, Y., Li, R. Y., Baba, S., *et al.* (2000) Cytomegalovirus infection of the central nervous system stem cells from mouse embryo: a model for developmental brain disorders induced by cytomegalovirus. *Lab. Invest.* **80**, 1373–1383
31. Bale, J. F., Jr., Blackman, J. A., and Sato, Y. (1990) Outcome in children with symptomatic congenital cytomegalovirus infection. *J. Child Neurol.* **5**, 131–136
32. Boppana, S. B., Pass, R. F., Britt, W. J., Stagno, S., and Alford, C. A. (1992) Symptomatic congenital cytomegalovirus infection: neonatal morbidity and mortality. *Pediatr. Infect. Dis. J.* **11**, 93–99
33. Crawley, J. N., Belknap, J. K., Collins, A., Crabbe, J. C., Frankel, W., Henderson, N., *et al.* (1997) Behavioral phenotypes of inbred mouse strains: implications and recommendations for molecular studies. *Psychopharmacology (Berl)* **132**, 107–124
34. Lee, S. H., Girard, S., Macina, D., Busa, M., Zafer, A., Belouchi, A., *et al.* (2001) Susceptibility to mouse cytomegalovirus is associated with deletion of an activating natural killer cell receptor of the C-type lectin superfamily. *Nat. Genet.* **28**, 42–45
35. Webb, J. R., Lee, S. H., and Vidal, S. M. (2002) Genetic control of innate immune responses against cytomegalovirus: MCMV meets its match. *Genes Immun.* **3**, 250–262
36. Sojka, D. K., Yang, L., and Yokoyama, W. M. (2019) Uterine natural killer cells. *Front. Immunol.* **10**, 960
37. Torres, L., and Tang, Q. (2014) Immediate-Early (IE) gene regulation of cytomegalovirus: IE1- and pp71-mediated viral strategies against cellular defenses. *Virol. Sin* **29**, 343–352
38. Ciocco-Schmitt, G. M., Karabekian, Z., Godfrey, E. W., Stenberg, R. M., Campbell, A. E., and Kerry, J. A. (2002) Identification and characterization of novel murine cytomegalovirus M112-113 (e1) gene products. *Virology* **294**, 199–208
39. van den Pol, A. N., Reuter, J. D., and Santarelli, J. G. (2002) Enhanced cytomegalovirus infection of developing brain independent of the adaptive immune system. *J. Virol.* **76**, 8842–8854
40. Kamiya, A., Kubo, K., Tomoda, T., Takaki, M., Youn, R., Ozeki, Y., *et al.* (2005) A schizophrenia-associated mutation of DISC1 perturbs cerebral cortex development. *Nat. Cell Biol.* **7**, 1167–1178
41. Marin, O. (2012) Brain development: the neuron family tree remodelled. *Nature* **490**, 185–186
42. Poduri, A., Evrony, G. D., Cai, X., and Walsh, C. A. (2013) Somatic mutation, genomic variation, and neurological disease. *Science* **341**, 1237758
43. Williamson, W. D., Desmond, M. M., LaFevers, N., Taber, L. H., Catlin, F. I., and Weaver, T. G. (1982) Symptomatic congenital cytomegalovirus. Disorders of language, learning, and hearing. *Am. J. Dis. Child* **136**, 902–905
44. Barker, G. R., Bird, F., Alexander, V., and Warburton, E. C. (2007) Recognition memory for objects, place, and temporal order: a disconnection analysis of the role of the medial prefrontal cortex and perirhinal cortex. *J. Neurosci.* **27**, 2948–2957
45. Weible, A. P., Rowland, D. C., Pang, R., and Kentros, C. (2009) Neural correlates of novel object and novel location recognition behavior in the mouse anterior cingulate cortex. *J. Neurophysiol.* **102**, 2055–2068
46. Aggleton, J. P., Albasser, M. M., Aggleton, D. J., Poirier, G. L., and Pearce, J. M. (2010) Lesions of the rat perirhinal cortex spare the acquisition of a complex configural visual discrimination yet impair object recognition. *Behav. Neurosci.* **124**, 55–68

47. Wilson, D. I., Langston, R. F., Schlesiger, M. I., Wagner, M., Watanabe, S., and Ainge, J. A. (2013) Lateral entorhinal cortex is critical for novel object-context recognition. *Hippocampus* **23**, 352–366
48. Brito, A. F., and Pinney, J. W. (2017) Protein-Protein interactions in virus-host systems. *Front. Microbiol.* **8**, 1557
49. Scheffner, M., Werness, B. A., Huibregtse, J. M., Levine, A. J., and Howley, P. M. (1990) The E6 oncoprotein encoded by human papillomavirus types 16 and 18 promotes the degradation of p53. *Cell* **63**, 1129–1136
50. Werness, B. A., Levine, A. J., and Howley, P. M. (1990) Association of human papillomavirus types 16 and 18 E6 proteins with p53. *Science* **248**, 76–79
51. Huibregtse, J. M., Scheffner, M., and Howley, P. M. (1991) A cellular protein mediates association of p53 with the E6 oncoprotein of human papillomavirus types 16 or 18. *EMBO J.* **10**, 4129–4135
52. Yeo-Teh, N. S. L., Ito, Y., and Jha, S. (2018) High-risk human papillomaviral oncogenes E6 and E7 target key cellular pathways to achieve oncogenesis. *Int. J. Mol. Sci.* **19**, 1706
53. Cosme-Cruz, R., Martinez, F. P., Perez, K. J., and Tang, Q. (2011) H2B homology region of major immediate-early protein 1 is essential for murine cytomegalovirus to disrupt nuclear domain 10, but is not important for viral replication in cell culture. *J. Gen. Virol.* **92**, 2006–2019
54. Salomoni, P., and Pandolfi, P. P. (2002) The role of PML in tumor suppression. *Cell* **108**, 165–170
55. Hsu, P. D., Lander, E. S., and Zhang, F. (2014) Development and applications of CRISPR-Cas9 for genome engineering. *Cell* **157**, 1262–1278
56. Tavalai, N., and Stamminger, T. (2011) Intrinsic cellular defense mechanisms targeting human cytomegalovirus. *Virus Res.* **157**, 128–133
57. Bieniasz, P. D. (2004) Intrinsic immunity: a front-line defense against viral attack. *Nat. Immunol.* **5**, 1109–1115
58. Xu, Y., Ahn, J. H., Cheng, M., apRhys, C. M., Chiou, C. J., Zong, J., *et al.* (2001) Proteasome-independent disruption of PML oncogenic domains (PODs), but not covalent modification by SUMO-1, is required for human cytomegalovirus immediate-early protein IE1 to inhibit PML-mediated transcriptional repression. *J. Virol.* **75**, 10683–10695
59. Muller, S., and Dejean, A. (1999) Viral immediate-early proteins abrogate the modification by SUMO-1 of PML and Sp100 proteins, correlating with nuclear body disruption. *J. Virol.* **73**, 5137–5143
60. Lee, H. R., Kim, D. J., Lee, J. M., Choi, C. Y., Ahn, B. Y., Hayward, G. S., *et al.* (2004) Ability of the human cytomegalovirus IE1 protein to modulate sumoylation of PML correlates with its functional activities in transcriptional regulation and infectivity in cultured fibroblast cells. *J. Virol.* **78**, 6527–6542
61. Brandon, N. J., and Sawa, A. (2011) Linking neurodevelopmental and synaptic theories of mental illness through DISC1. *Nat. Rev. Neurosci.* **12**, 707–722
62. Sawamura, N., Ando, T., Maruyama, Y., Fujimuro, M., Mochizuki, H., Honjo, K., *et al.* (2008) Nuclear DISC1 regulates CRE-mediated gene transcription and sleep homeostasis in the fruit fly. *Mol. Psychiatry* **13**, 1138–1148
63. Ahn, J. H., Brignole, E. J., 3rd, and Hayward, G. S. (1998) Disruption of PML subnuclear domains by the acidic IE1 protein of human cytomegalovirus is mediated through interaction with PML and may modulate a RING finger-dependent cryptic transactivator function of PML. *Mol. Cell Biol.* **18**, 4899–4913
64. Scherer, M., Klingl, S., Sevvana, M., Otto, V., Schilling, E. M., Stump, J. D., *et al.* (2014) Crystal structure of cytomegalovirus IE1 protein reveals targeting of TRIM family member PML *via* coiled-coil interactions. *PLoS Pathog.* **10**, e1004512
65. Hayashi-Takagi, A., Takaki, M., Graziane, N., Seshadri, S., Murdoch, H., Dunlop, A. J., *et al.* (2010) Disrupted-in-Schizophrenia 1 (DISC1) regulates spines of the glutamate synapse *via* Rac1. *Nat. Neurosci.* **13**, 327–332
66. Ishizuka, K., Kamiya, A., Oh, E. C., Kanki, H., Seshadri, S., Robinson, J. F., *et al.* (2011) DISC1-dependent switch from progenitor proliferation to migration in the developing cortex. *Nature* **473**, 92–96
67. Mao, Y., Ge, X., Frank, C. L., Madison, J. M., Koehler, A. N., Doud, M. K., *et al.* (2009) Disrupted in schizophrenia 1 regulates neuronal progenitor proliferation *via* modulation of GSK3beta/beta-catenin signaling. *Cell* **136**, 1017–1031
68. Narayan, S., Nakajima, K., and Sawa, A. (2013) DISC1: a key lead in studying cortical development and associated brain disorders. *Neuroscientist* **19**, 451–464
69. Li, X. J., Liu, X. J., Yang, B., Fu, Y. R., Zhao, F., Shen, Z. Z., *et al.* (2015) Human cytomegalovirus infection dysregulates the localization and stability of NICD1 and Jag1 in neural progenitor cells. *J. Virol.* **89**, 6792–6804
70. Corbin, J. G., Gaiano, N., Juliano, S. L., Poluch, S., Stancik, E., and Haydar, T. F. (2008) Regulation of neural progenitor cell development in the nervous system. *J. Neurochem.* **106**, 2272–2287
71. Perles, Z., Moon, S., Ta-Shma, A., Yaacov, B., Francescatto, L., Edvardson, S., *et al.* (2015) A human laterality disorder caused by a homozygous deleterious mutation in MMP21. *J. Med. Genet.* **52**, 840–847
72. Rolland, M., Li, X., Sellier, Y., Martin, H., Perez-Berezo, T., Rauwel, B., *et al.* (2016) PPARgamma is activated during congenital cytomegalovirus infection and inhibits neuronogenesis from human neural stem cells. *PLoS Pathog.* **12**, e1005547
73. Wu, C. C., Jiang, X., Wang, X. Z., Liu, X. J., Li, X. J., Yang, B., *et al.* (2018) Human cytomegalovirus immediate early 1 protein causes loss of SOX2 from neural progenitor cells by trapping unphosphorylated STAT3 in the nucleus. *J. Virol.* **92**, e00340-18
74. Li, K., Wang, F., Yang, Z. N., Cui, B., Li, P. P., Li, Z. Y., *et al.* (2020) PML-RARalpha interaction with TRIB3 impedes PPARgamma/RXR function and triggers dyslipidemia in acute promyelocytic leukemia. *Theranostics* **10**, 10326–10340
75. Cloarec, R., Bauer, S., Teissier, N., Schaller, F., Luche, H., Courtens, S., *et al.* (2018) In utero administration of drugs targeting Microglia improves the neurodevelopmental outcome following cytomegalovirus infection of the Rat fetal brain. *Front. Cell Neurosci.* **12**, 55
76. Tang, Q., and Maul, G. G. (2003) Mouse cytomegalovirus immediate-early protein 1 binds with host cell repressors to relieve suppressive effects on viral transcription and replication during lytic infection. *J. Virol.* **77**, 1357–1367
77. Ozeki, Y., Tomoda, T., Kleiderlein, J., Kamiya, A., Bord, L., Fujii, K., *et al.* (2003) Disrupted-in-Schizophrenia-1 (DISC-1): mutant truncation prevents binding to NudE-like (NUDEL) and inhibits neurite outgrowth. *Proc. Natl. Acad. Sci. U. S. A.* **100**, 289–294
78. Tsutsui, Y., Kosugi, I., and Kawasaki, H. (2005) Neuropathogenesis in cytomegalovirus infection: indication of the mechanisms using mouse models. *Rev. Med. Virol.* **15**, 327–345
79. Peter, C. J., Saito, A., Hasegawa, Y., Tanaka, Y., Nagpal, M., Perez, G., *et al.* (2019) In vivo epigenetic editing of Sema6a promoter reverses transcallosal dysconnectivity caused by C11orf46/Arl14ep risk gene. *Nat. Commun.* **10**, 4112
80. Hikida, T., Jaaro-Peled, H., Seshadri, S., Oishi, K., Hookway, C., Kong, S., *et al.* (2007) Dominant-negative DISC1 transgenic mice display schizophrenia-associated phenotypes detected by measures translatable to humans. *Proc. Natl. Acad. Sci. U. S. A.* **104**, 14501–14506